THE INTERNATIONAL JOURNAL OF MEDICAL ROBOTICS AND COMPUTER ASSISTED SURGERY
Int J Med Robotics Comput Assist Surg 2010; **6**: 194–201.
Published online 17 March 2010 in Wiley InterScience (www.interscience.wiley.com). **DOI:** 10.1002/rcs.306

ORIGINAL ARTICLE

Remote-controlled vascular interventional surgery robot

Tianmiao Wang
Dapeng Zhang*
Liu Da

Beijing University of Aeronautics and Astronautics Robotics Institute, Beijing, People's Republic of China

*Correspondence to: Dapeng Zhang, Room A 318, New Teaching-Research Building, 37 Xueyuan Road, Haidian District, Beijing, People's Republic of China.
E-mail: zdp80@yahoo.com.cn

Accepted: 3 February 2010

Abstract

Background Conventional vascular interventional surgery (VIS) is manually performed under fluoroscopic guidance, requiring lead protection for the surgeons. A remote-control vascular interventional surgery robot (VISR) which can remotely, safely and precisely perform VIS would have clear advantages.

Methods Our robot adopts a master–slave structure. The surgeon sits at the master site, sending controlling instructions to the robot fixed at the slave site, then the robot translates these instructions into catheter motion. The robotic mechanism consists of a supporting manipulator and a catheter navigator; the former adjusts the robot's spatial position, while the latter controls the translation and rotation of the catheter. A 3D vascular model is reconstructed so that the surgeon can perform surgical planning easily. In addition, the tactile force between catheter tip and blood vessel is measured, which prevents the surgeon damaging delicate vessels. In glass model and animal experiments, the surgeon remotely controlled VISR, which inserted a catheter into predefined targets, and the robotic surgery time was measured.

Results The robot was initially tested on a transparent glass vascular model. Under robotic manipulation, the catheter can enter an arbitrary branch of the vascular model and catheter motion can meet the requirements of clinical VIS. Then robotic surgery was performed successfully in an adult dog. Surgery time to access each of the five targets, viz. renal artery, left atrium, right atrium, left ventricle and right ventricle, was measured. Compared with conventional manual surgery, robotic surgery time is a little longer.

Conclusions The experiments show the feasibility and safety of the VISR to facilitate navigation, position precisely and control catheters to specific regions. The VISR system offers surgeon radiation safety and minimizes surgeon-based error. Copyright © 2010 John Wiley & Sons, Ltd.

Keywords remote control; vascular intervention; surgery robot; mechanism and control; image navigation

Introduction

Vascular interventional surgery (VIS) is a minimally invasive therapy for treatments of vascular disease and tumours. During conventional VIS, the surgeon makes an incision in the groin through which a catheter can be inserted. Then, under fluoroscopic guidance, the surgeon directs the catheter towards the target by manipulating the catheter tail. The catheter is then used as a conduit for passing therapeutic devices (stent or balloon) or injecting

drugs. Compared to open surgery, VIS has multiple advantages, including minimal haemorrhage and a need for only local anaesthesia. However, the surgeons may suffer from radiation sickness, including injury to skin, eyes, etc., even when protective measures have already been taken (1–3). Additionally, some human factors, such as operator skill, may decide the success or otherwise of VIS. Introducing a robot into VIS is one solution that can effectively solve these problems. Teleoperation technology is applied to control the robot, so the surgeon can avoid X-ray irradiation. Also, the robot can quantify catheter motion, which decreases artificial influence on operation quality.

Several groups have been developing vascular interventional surgery robots (VISRs) in recent years. The Niobe Magnetic Navigation System (Stereotaxis, USA) was designed for cardiac intervention, allowing surgeons to more effectively navigate guide wire, catheter and other magnetic interventional devices (4). The NaviCath system (Haifa, Israel) was devised to execute interventional catheterization procedures from a remote location in a precise and well-controlled fashion. The system includes a bedside unit and an operator control unit. The former is installed on the operating table, controlling the guide wire for axial and rotational movements. The latter locates away from the patient bed, comprising a computerized touchscreen-controlled console and a joystick (5). The Sensei robotic catheter control system (CCS), designed by the Hansen Medical Co., has been developed to facilitate control and precise positioning of catheter within the cardiovascular system. The surgeon controls the CCS at the master console, using the input device to direct the catheter tip, and fluoroscopic images are displayed, providing immediate feedback to the surgeon (6). A catheter operating robot system (CORS) for vascular neurosurgery has been developed by Shuxiang Guo. CORS also adopts a master–slave structure. At the master site, the surgeon manipulates the robot far away from the slave site (7).

However, the VISR mentioned above have several disadvantages. First, the dexterity of the mechanism needs to be improved further. To allow the catheter to enter blood vessels successfully, the surgeon frequently needs to adjust the posture of the robotic. So robotic mechanism should be dexterous enough to facilitate surgeon operations. Second, the surgeon manipulates the robot under the guidance of two-dimensional (2D) digital subtraction angiography (DSA) projection images. Due to the problem of vessel overlap and foreshortening, 2D projection images may lose a significant amount of the information of three-dimensional (3D) blood vessels, and the volume and orientation of the vasculature can not be determined precisely by several projection images. Surgeons have to reconstruct 3D vasculature in their minds. So it is difficult for surgeons to operate the robot, especially for novices. Third, robots can not provide surgeons with contact forces between the blood vessels and catheter. During conventional manual VIS, surgeons adjust catheter motion depending on the moving resistance of the catheter. However, the surgeon can not touch the catheter in robotic surgery, i.e. only visual feedback is provided.

We designed a remote-control VISR for cardiovascular intervention. Compared with the robots mentioned above, our robot has three improvements. First, the robotic mechanism consists of two parts, a supporting manipulator and a catheter navigator. The former sets the position of the catheter navigator; the latter navigates the catheter according to the surgeon's instructions, which can increase robotic dexterity greatly. Second, the image navigation system reconstructs a 3D vascular model from the 2D projection images, so the surgeon can diagnose pathological changes easily and control the catheter quantitatively, which efficiently reduces surgery risk due to artificial reasons. Third, we present a novel piezoelectric sensor to measure the contact force between the catheter and the arterial wall. The tactile force is transmitted to the surgeon's hand, which prevents the surgeon from damaging the blood vessels.

This paper is organized as follows: in the next section, we describe key technologies involved in our VISR – mechanism and control, image navigation and feedback force. The experimental results are presented in the next section. Finally, we discuss our conclusions and suggest future work.

Materials and Methods

To protect surgeons from X-ray exposure, our VISR system also adopts a master–slave structure, as illustrated in Figure 1. First, the surgeon extracts the catheter spatial

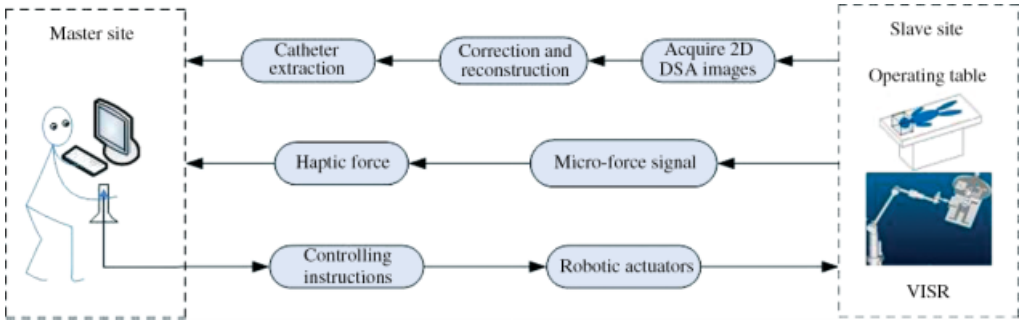

Figure 1. System structure of remote-control VISR

DOI: 10.1002/rcs

position and reconstructs a 3D vascular model from acquired DSA images, which can realize the integrated display of catheter and blood vessels. Second, based on position information of the catheter within the blood vessels, the surgeon sends controlling instructions to a robot fixed on the operation table. Then the robot translates these instructions into catheter motions. Third, the surgeon can adjust catheter motions according to haptic forces between the catheter and the blood vessels, measured by a microsensor. It mainly involves three key technologies: mechanism and control, image navigation and feedback force. These are detailed in the following sections.

Mechanism and control

During conventional VIS, surgeons generally push or pull the catheter axially within the vascular network. When entering a vascular branch or moving with difficulty, the catheter will be rotated to change the direction of motion. VISR therefore needs to simulate manual operations and achieve catheter axial (advance and retract) and rotational movements. Therefore, in order to control the catheter neatly, we present a novel robotic mechanism consisting of two parts, a supporting manipulator and a catheter navigator, as shown in Figure 2. The supporting manipulator is constituted by a five degree of freedom (DOF) passive hydraulic mechanism, which can be locked to an arbitrary posture. During robotic VIS, the surgeon manually adjusts the hydraulic manipulator to an appropriate position so that the catheter, clamped by the catheter navigator, is directed along the vein.

The catheter navigator, fixed at the tip of the supporting manipulator, controls catheter axial and rotational motions, as shown in Figure 3. The principles of the catheter navigator are illustrated in Figure 4. The catheter is clamped by rollers 1 and 2. Axial translation is implemented by stepping motor 2 driving rollers 1 and 2. The distance between the two rollers is adjustable, so the robot can drive different kinds of catheter. When the robot does not work, the surgeon can remove the catheter quickly and switch to manual operation. Additionally, two rollers are fixed onto a passive gear, so when stepping motor 1 drives an active gear, the catheter is also rotated.

Figure 2. Mechanics structure of VISR

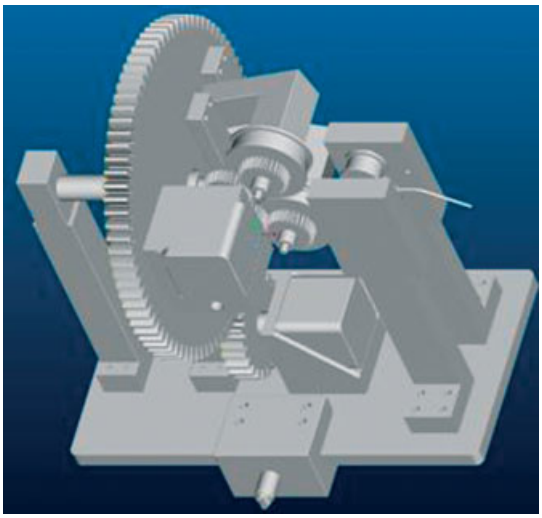

Figure 3. Structure of the catheter navigator shown in Figure 4. The catheter is clamped by rollers 1 and 2. Axial translation is implemented by stepping motor 2 driving rollers 1 and 2. The distance between the two rollers is adjustable, so the robot can drive different kinds of catheter. When the robot does not work, the surgeon can take out the catheter quickly and switch to manual operation. Additionally, the two rollers are fixed onto a passive gear, so when stepping motor 1 drives the active gear, the catheter is also rotated

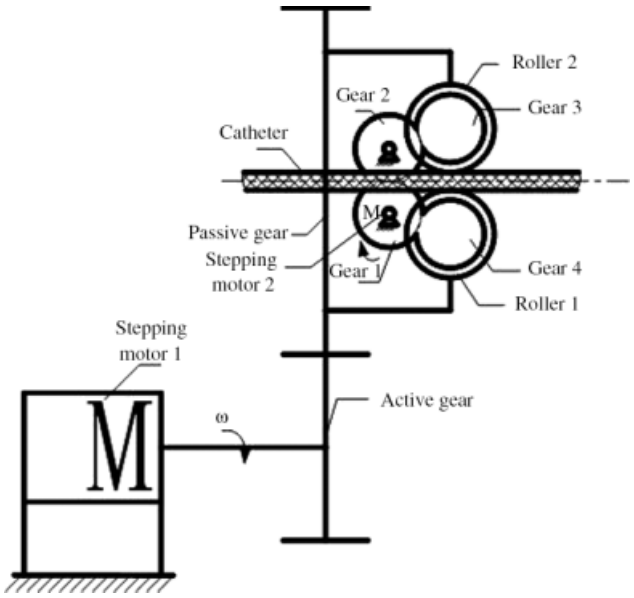

Figure 4. Principles of the catheter navigator

To implement remote real-time manipulation, a network layer is designed for transmission between the master and slave sites. Operation signals on the master site are encoded into protocol-based messages and sent to the slave site. The messages are decoded at the slave site to drive the robot.

DOI: 10.1002/rcs

Image navigation

Generally, the surgeon manipulates robot under 2D real-time projection images. However, when the catheter needs to turn into a vascular branch, it is difficult for the surgeon to determine the position and orientation of the catheter within the tortuous vasculature. This results in prolonged X-ray exposure for the patient and the medical staff. In this study, 3D representation of the catheter and blood vessels has been introduced to accomplish accurate robotic navigation. First, the DSA machine should be calibrated so as to correct the acquired 2D projection images. Second, the catheter and vascular centrelines are extracted in the calibrated images. Then the catheter position and vascular cross-section are decided by using the epipolar concept, calculating by angular distance of the two projections. Vascular complexity decides the projection number used for reconstructing the 3D model. Third, the catheter and blood vessels are reconstructed and the surgeon sends controlling instructions according to the relative position of the catheter within the blood vessels.

DSA calibration and image correction

To reconstruct the 3D catheter and vascular model accurately, we needed to calibrate the DSA machine in order to obtain internal and external parameters. These parameters were required for image correction, due to various types of distortion of acquired projection images (8–10). In this study, the Tsai method was adopted to calibrate the 3D rotational angiography facility (11). The distortions were measured using a Cartesian grid phantom, consisting of double-layer spaced grid points, and the phantom was mounted in front of the detector plane of an image intensifier, as shown in Figure 5. The relationship between the imaged grid points and the real Cartesian grid was determined by modelling the distortions along the x and y axes. The correction was performed with interpolation at the subpixel level and the correction method was accurate and reproducible. We performed the calibration procedure in each direction off-line and stored positional information of the focal spots and correction parameters of different orientations.

3D vascular reconstruction from two projection images

Reconstruction of a 3D vascular model consisted of three steps. First, the vascular centreline in the 2D projection image had to be extracted. In this study, the vascular centreline was identified manually; the surgeon indicated several points near the centreline in each of the selected projections, the number of points depending on the vascular structure being segmented, with tortuous regions requiring more points. Then the centreline was created by a polynomial interpolation of the manually determined

Figure 5. Physical set-up of the calibration phantom

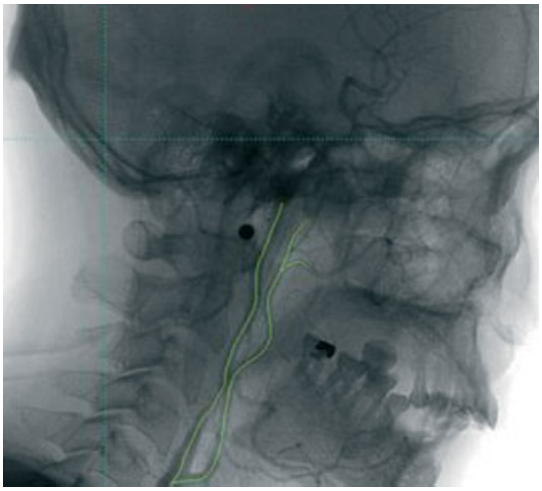

Figure 6. Extraction of the vascular centreline

centreline points, as shown in Figure 6. Second, in order to reconstruct a point $P^{3D} \in R^3$ in space from two projections, the corresponding image point of $P_A \in A$ in projection B had to be decided, as shown in Figure 7. F_A and F_B express the X-ray source in two different orientations and A and B are the corresponding image-intensifier planes, respectively. The correspondences of the image points can be solved using epipolar constraint. Given a point P_A in projection A, its corresponding point in projection B must lie on the generated epipolar line. The epipolar line is given by the intersection of the plane H, which is defined by the point P_A, F_A and F_B and the projection B. Then the point P_B was determined by searching along the epipolar line in projection B. The spatial position of P^{3D} was then calculated by a simple intersection of the lines from the points on the projections to their respective X-ray source.

Third, 3D reconstruction of the vascular radius was performed. As illustrated in Figure 8, for each 2D centreline point P_{ji}^{2D}, the 2D edge-points E_{ji}^{l} and E_{ji}^{r} of the centreline points were automatically estimated in the projections, using scale–space techniques, as described in (12–14). The points E_{ji}^{l}, E_{ji}^{r} and F_j define a triangle; it is clear that the borders of the 3D blood vessel must intersect the lines $F_j E_{ji}^{l}$ and $F_j E_{ji}^{r}$, respectively. When

DOI: 10.1002/rcs

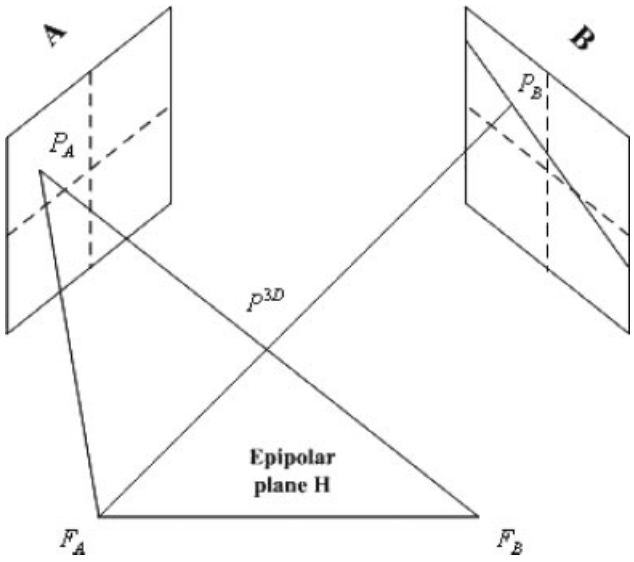

Figure 7. 3D point reconstruction from two projections

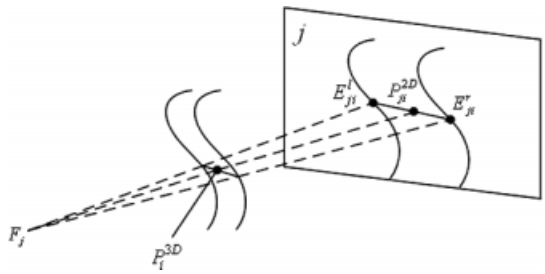

Figure 8. Schematic diagram of vascular projection

using two projections (j and k), an elliptical cross-section can be employed, as illustrated in Figure 9. In order to derive a more realistic shape of the 3D blood vessel, several projections are needed (15–16). However, multiple projections will increase the X-ray radiation to patients, so we prefer to reconstruct the 3D vascular and catheter model from two projections. The angle between two projections should be chosen with minimal foreshortening and minimal vessel overlap relative to the segment of interest, i.e. the surgeon selects two projections according to the vascular trend.

The catheter reconstruction is similar to the vascular centreline, then the catheter is displayed within the blood vessels. We therefore obtained the exact positional information, including the distance and orientation angle between the catheter tip and next branch. According to this positional information, the surgeon sends controlling commands to the robot.

Feedback force

During conventional VIS, the surgeon adjusts catheter motion according to the feedback force at the catheter tail. However, in robotic surgery the surgeon can not touch the catheter, and the catheter tip sometimes may result in vascular rupture during clinical operation (17). In

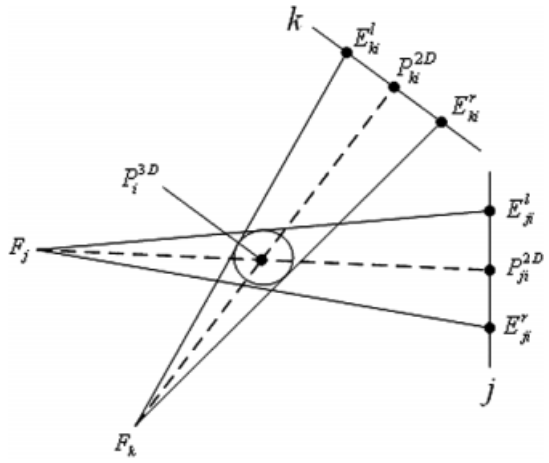

Figure 9. 3D radius calculation from two projection images

order to protect blood vessels from damage during VISR, a miniature piezoelectric sensor fixed on the catheter tip is introduced to detect the tactile force between the catheter tip and the arterial wall, and feedback force that exceeds a threshold causes the robotic system to stall. The measured feedback force is transmitted in real time to the surgeon via a haptic interface device, Omega 6 (provided by Force Dimension Co.).

Polyvinylidene fluoride (PVDF) film is a semicrystalline polymer and has a strong piezoelectricity, so PVDF film was used in our microsensor to detect the contact force. We used glue to affix the PVDF film to the catheter, and the rubber film insulated the PVDF film from the blood, as shown in Figure 10. When external force is applied on the PVDF film, charges of opposite polarity accumulate on both sides. Then the charges on the PVDF film are transmitted by wires to a signal amplifier, so that output voltages can be detected easily (7). Therefore, we established a link between the external force and the output signals. Additionally, feedback force is proportionally adjustable according to the feelings of the surgeon. We invited three experienced interventional radiologists (Navy Hospital, Beijing, China), who had performed VIS for >10 years, to test and evaluate the measured feedback force. Their evaluation was that when the catheter tip collides with arterial walls, the feedback force provided by the miniature sensor can give the surgeon real resistance, which can prevent the surgeon from injuring the blood vessels.

Experiments

The master site, located away from the patient bed, comprises a PC (dual-processor Intel Xeon, 3.0 GHz) with double displays and haptic interface device Omega, as shown in Figure 11. The real-time 2D projection images are shown on one display and the 3D vascular modelling and surgical planning are shown on the other display. Under the guidance of images and feedback force, the surgeon sits at the master site and sends controlling instructions to the robot fixed on the operating bed.

DOI: 10.1002/rcs

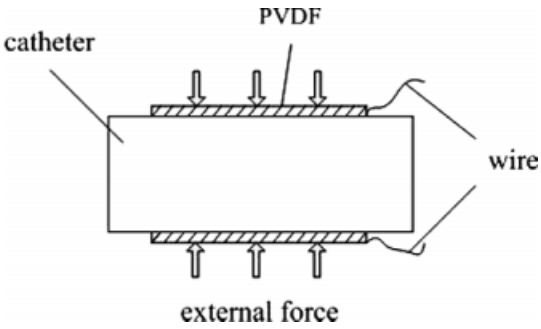

Figure 10. Schematic diagram of the microsensor

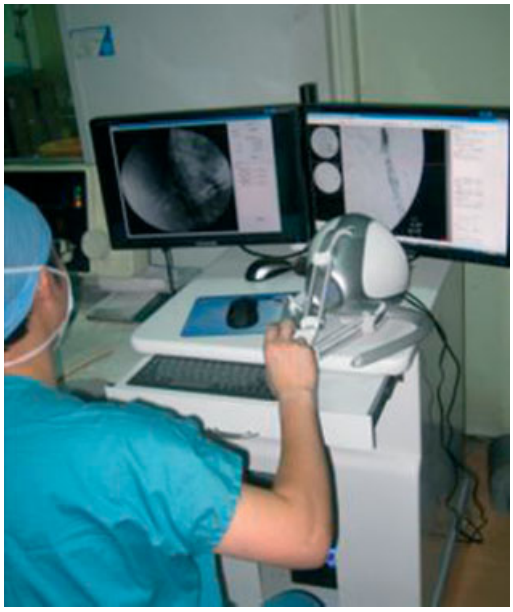

Figure 11. Robotic control console at the master site

Figure 12. Glass model experiment scene

The robot was initially tested on a transparent glass vascular model filled with distilled water to verify the impact of catheter speed on the motion accuracy, as illustrated in Figure 12. The robot controls catheter movement at different speeds, then compares the actual moving distance with the theoretical value.

From the structural chart of the catheter navigator shown in Figure 4, the theoretical value of catheter translation, S, is calculated using equation (1):

$$S = \frac{p\pi d}{N}. \tag{1}$$

where p is the pulse number that the operator sends to the stepping motor, d denotes the diameter of roller 1, and N expresses the required pulses when roller 1 rotates for a period. From equation (1), we can clearly see that the theoretical value of catheter translation is only related to the received pulse counts.

After the propagation of the catheter, a series of 3D rotational angiography images are acquired using a digital subtraction angiography (DSA) machine (GE LCV + 3000). The actual moving distance of the catheter is obtained from the angiography images using the 3D reconstruction method mentioned above.

The robot manipulated catheter motion at different speeds to test the impact of speed on translation precision. The stepping motor is given 2×10^4 pulses, and the theoretical value of catheter translation calculated by equation (1) is 157.5 mm. We repeated the manipulation 10 times at each speed and the experimental results are shown in Figure 13. When stepping motor emits 2–4 pulses/ms, the error band of catheter motion is $<$0.5 mm, i.e. the actual moving distance varies in the range 157–158 mm. However, while the emitting speed of pulses is $>$4 pulses, or $<$2 pulses/ms, the actual moving distance deviates from the theoretical value much more, as indicated by an asterisk. Additionally, when the stepping motor emits 2–4 pulses/ms the moving speed of the catheter is 10–25 mm/s, which meets the clinical demands of VIS.

Then the robot was tested in animals, which was reviewed and approved by the Institutional Animal Care at the Navy Hospital, Beijing. As illustrated in Figure 14, an adult dog weighing $\geq$ 20 kg was studied. Following standard and approved protocols, the dog was anaesthetized to ensure that discomfort, distress, pain and injury were limited to that which was unavoidable. The predefined targets included renal artery, left atrium, right atrium, left ventricle and right ventricle. The

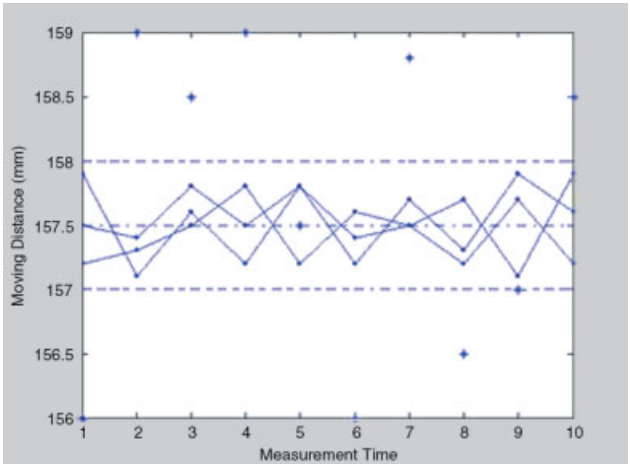

Figure 13. Moving distance according to different speeds

DOI: 10.1002/rcs

Figure 14. Animal experiment scene

robot inserted 1.5 mm diameter catheters into predefined targets.

Results and Discussion

We initially tested the influence of catheter speed on accuracy. When the stepping motor received 2–4 pulses/ms, the error of catheter motion was <0.5 mm. This speed met the requirements of clinical VIS. Based on the accuracy test on the glass model, the animal experiment was carried out to access the cardiovascular and renal artery. Under the image and feedback-force guidance, the surgeon repeated conventional manual and robotic surgery five times, respectively. The average times taken are shown in Table 1, from which we can clearly see that robotic surgery needs more time than conventional surgery, which is partly related to the operator's experience with the new robotic system.

Table 1. Time comparison between conventional and robotic surgery

Surgical site	Conventional surgery time (min)	Robotic surgery time (min)
Renal artery	4.5	6
Left atrium	8	10.5
Right atrium	5	6
Left ventricle	6.5	8
Right ventricle	5	7.5

Conclusions and Future Work

We propose a remote-control VISR to achieve transparent glass model and animal experiments. The experiments showed that the catheter could be easily manipulated through the vascular branches and the angioplasty device could be easily positioned at the required locations.

Our VISR mainly involves three key technologies: mechanism and control, image navigation and feedback force. First, to increase mechanism dexterity, robot consists of two parts, a supporting manipulator and a catheter navigator. The former is used to support and adjust robotic posture according to the surgeon's demands, so that the catheter can move flexibly. The latter controls catheter axial and rotational movements. Second, a robotic navigation system based on acquired 2D projection images has been presented, which reconstructs the 3D catheter position and a vascular model during VIS. The surgeon can therefore make surgical planning according to the relative position of the catheter within the blood vessels, which reduces surgical complexity and improves safety. Third, a novel piezoelectric sensor is introduced to measure the tactile force between the catheter and the blood vessel. Feedback force is transmitted to the surgeon by a haptic interface device, which can effectively prevent the surgeon from damaging the blood vessels.

The potential advantages of our remote-controlled VISR can be summarized as:

- Avoiding X-ray radiation of the surgeon and providing a convenient working environment.
- Quantifying catheter motion, which reduces surgical risk due to artificial reasons.
- Measuring the contact force between the arterial wall and the catheter tip, which improves surgical safety.

However, some limitations exist in our robot. The system is applied to relatively simple lesions, and robotic surgery time is a little longer than manual operation, which can be partially related to the operator's experience with the new robotic system. These problems can be solved in the future by upgrading the robotic system and improving the operator's skill. We also need to revise the robotic mechanism so that it can control guide-wire movement.

Acknowledgements

The authors would like to thank Shuxiang Guo from Kagawa University, Japan, for his guidance regarding the microsensor. This work was supported by the National High Technology Projection 'Research on Vascular Interventional Robot' (Grant No. 2007AA04Z246) and the National Nature Science Foundation (Grant No. 60705033).

References

1. http://priory.com/med/radiation.htm.

2. den Boer A, de Feijter PJ, Serruys PW. Real-time quantification and display of skin radiation during coronary angiography and intervention. *Am Heart Assoc* 2001; **104**: 1779–1784.
3. Hidajat N, Wust MDP. Radiation risks for the radiologist performing transjugular intrahepatic portosystemic shunt. *Br J Radiol* 2006; **79**: 483–486.
4. Faddis MN, Lindsay BD. Magnetic catheter manipulation. *Coronary Art Dis* 2003; **14**: 25–27.
5. Beyar R, Gruberg L, Deleanu D, *et al*. Remote-control percutaneous coronary interventions. *J Am Coll Cardiol* 2006; **47**: 296–300.
6. Saliba W, Cummings J, Oh S, *et al*. Novel robotic catheter remote control system: feasibility and safety of trans-septal puncture and endocardial catheter navigation. *J Cardiovasc Electrophysiol* 2006; **17**: 1102–1105.
7. Guo S, Kondo H, Wang J, *et al*. A new catheter operating system for medical applications. In Proceedings of the IEEE/ICME International Conference on Complex Medical Engineering, 23–27 May 2007; 111–115.
8. Wiesent K, Barth K, Navab N, *et al*. Enhanced 3D reconstruction algorithm for C-arm systems suitable for interventional procedures. *IEEE Trans Med Imag* 2000; **19**: 391–403.
9. Rougee A, Picard C, Ponchut C, *et al*. Geometrical calibration of X-ray imaging chains for three-dimensional reconstruction. *Comput Med Imag Graph* 1993; **17**: 295–300.
10. Chung HT, Kim DG. Distortion correction for digital subtraction angiography imaging: PC based system for radiosurgery planning. *Comput Methods Programs Biomed* 2003; **71**: 165–173.
11. Roger Y. TSAI: a versatile camera calibration technique for high-accuracy 3D machine vision metrology using off-the-shelf TV cameras and lenses. *IEEE J Robotics Autom* 1987; **4**: 323–344.
12. Lorenz C. Multi-scale line segmentation with automatic estimation of width contrast and tangential direction in 2D and 3D medical images. In Proceedings of Computer Vision, Virtual Reality and Robotics in Medicine and Medical Robotics and Computer-Assisted Surgery CVRMed–MRCAS 1997; pp. 233–242.
13. Lorenz C, Buzug TM, Fassnacht C, *et al*. A multi-scale line filter with automatic scale selection on the Hessian matrix for medical image segmentation. Proceedings of the International Conference on Scale-Space, 1997; 152–163.
14. Chan RC, Karl WC, Lees RS. A new model-based technique for enhanced small-vessel measurements in X-ray cine-angiograms. *IEEE Trans Med Imag* 2000; **19**: 243–255.
15. Movassaghi B, Rasche V, Grass M, *et al*. A quantitative analysis of 3D coronary modeling from two or more projecion images. *IEEE Trans Med Imag* 2004; **23**: 1517–1531.
16. Chen SJ, Carroll JD. 3D reconstruction of coronary arterial tree to optimize angiographic visualization. *IEEE Trans Med Imag* 2000; **19**: 318–336.
17. Yeo KK, Rogers JH. Side branch access. *Cardiac Intervent Today* 2009; March: 22–24.